Density-functional investigation of magnetism in δ-Pu

Per Söderlind, Alex Landa, and Babak Sadigh
Lawrence Livermore National Laboratory, University of California, P.O. Box 808, Livermore, California 94550
(Received 26 July 2002; published 27 November 2002)

We present density-functional results of δ-Pu obtained from three electronic-structure methods. These methods have their individual strengths and are used in combination to investigate the magnetic and crystal stability of δ-Pu. An all-electron, full potential linear muffin-tin orbitals (FPLMTO) method, that includes corrections for spin-orbit coupling and orbital-polarization effects, predicts δ-Pu to be an antiferromagnet at zero temperature with a volume and a bulk modulus in very good agreement with experiment. The site-projected magnetic moment is smaller than expected ($\sim 1.5\ \mu_B$) due to large cancellation of spin and orbital moments. These calculations also predict a mechanical instability of antiferromagnetic (AF) δ-Pu. In addition, techniques based on the Korringa-Kohn-Rostoker (KKR) method within a Green's-function formalism and a projector augmented wave (PAW) method predict the same behavior of δ-Pu. In order to study disordered magnetism in δ-Pu, the KKR Green's-function technique was used in conjunction with the disordered local-moment model, whereas for the FPLMTO and PAW methods this was accomplished within the special quasirandom structure model. While AF δ-Pu remains mechanically unstable at lower temperatures, paramagnetic δ-Pu is stabilized at higher temperatures where disordered magnetic moments are present and responsible for the crystal structure, the low density, and the low bulk modulus of this phase.

DOI: 10.1103/PhysRevB.66.205109 PACS number(s): 71.15.Mb, 64.10.+h, 71.27.+a, 75.10.Lp

I. INTRODUCTION

Plutonium metal is located in the series of actinides in the periodic table of elements, does not occur naturally, but is man-made for nuclear power purposes. With the practical importance of this material it is essential to understand its fundamental properties. Pu, however, is an extremely complicated metal with a most anomalous phase diagram[1] showing as many as six distinct phases, see Fig. 1. The ground-state α-Pu is relatively well understood with cohesive and structural properties governed by narrow $5f$ bands containing about five electrons. Density-functional electronic-structure calculations predict the density, bulk modulus, crystal structure, thermal expansion, and magnetic properties in good agreement[2] with experiment. This gives us strong confidence in density-functional theory (DFT) because many of the above properties are in fact quite anomalous and unexpected for a metallic element. Also, the fact that the close-neighbor metal, uranium, is very accurately described by DFT including delicate details of the crystal structure as well as elastic constants[3] supports this notion. This ground-state α phase is, however, very brittle and not suitable for engineering applications whereas the face-centered-cubic (fcc) δ-Pu is more ductile and useful in practice. The pure Pu δ phase is stable at about 600 K but can be alloyed with a small amount of, for example, Ga, Al, Sc, Ce, or Am which will stabilize δ-Pu at lower temperatures.

Although technologically more important, δ-Pu and its alloys are less understood than α-Pu. For instance, DFT, which relatively accurately describes α-Pu, underestimates the volume of δ-Pu by about 20%, overestimates the bulk modulus by 300%, and predicts negative elastic constants.[4] To remedy this, several *ad hoc* techniques[5–7] have been applied to δ-Pu attempting to reproduce experimental data. The most recent publications are based on the dynamical mean-field picture of Savrasov *et al.*[8,9] and conventional DFT with spin and orbital corrections.[4] Both these approaches reproduce several properties of δ-Pu but the former theory is not accurate enough to deal with the α phase of Pu. The latter calculations[4] accurately describe α-Pu but predict ordered magnetism in δ-Pu which has not been confirmed by experiment.

In the present paper we follow the ideas put forward by Söderlind[4] but expand the investigation to study several magnetic configurations of δ-Pu including models for disordered magnetic structure. Also, the structural stability of the fcc δ phase is investigated. To this end, full potential linear muffin-tin orbitals (FPLMTO), Korringa-Kohn-Rostoker

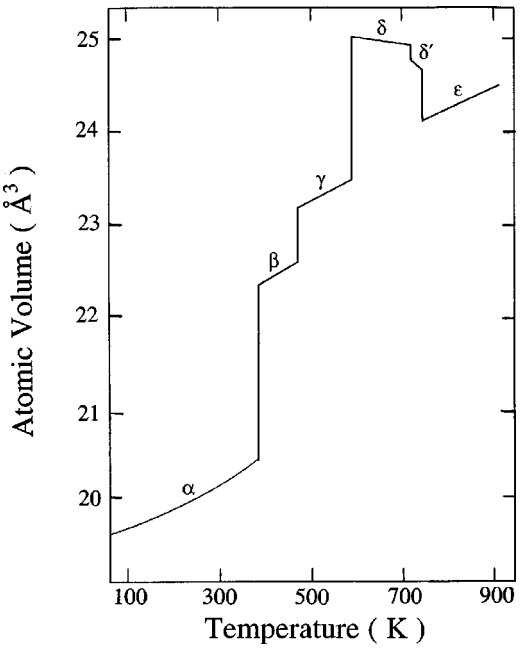

FIG. 1. The experimental (Ref. 1) phase diagram of plutonium.

(KKR), and projector augmented wave (PAW) methods have been employed and these are described in Sec. II. The remainder of the paper is organized as follows. We present our results from studying stability of the magnetic structures in Sec. III and structural stabilities in Sec. IV. Also, in an attempt to compare our electronic structure with experiment and other models, we present the calculated electronic density of states in Sec. V. Lastly, in Sec. VI, we offer our conclusions and ideas for future work.

II. COMPUTATIONAL DETAILS

In this paper we calculate the electronic structure of δ-Pu using a combination of three methods which each have distinct advantages. The most accurate method, which is also the most computer intensive, is an all-electron FPLMTO method that will be described first. Second, we give the details of a KKR method which is computationally efficient with the added advantage of being able to treat ordered and disordered alloys within the coherent-potential approximation (CPA). This latter feature enables the disordered local-moment (DLM) method to be used to describe disordered magnetism without the use of a super cell. Lastly, we describe a PAW method with a plane-wave basis set, which enables efficient calculations of forces and relaxations. These three methods all rely upon the density-functional theory with recent approximations to the electron exchange/correlation functional. In addition, the FPLMTO method include corrections due to spin-orbit coupling and orbital polarization.

A. FPLMTO

The parameters of the calculations are the same as those given earlier,[4] but the more important details are repeated here. This electronic-structure method is an implementation of density-functional theory as applied for a bulk material.[10] It is a first-principles method; no experimental numbers are used in the calculations except for the nuclear charge which is 94 for Pu. The approximations in this approach are limited to the approximation of the exchange/correlation energy functional, cutoffs in the expansion of basis functions, *k*-point sampling in integrations over the Brillouin zone (BZ), and the Born-Oppenheimer approximation. For the exchange/correlation approximation we used the generalized gradient approximation (GGA),[11] which has proven to be better for *f*-electron metals than the more commonly used local-density approximation (LDA). Spin-orbit coupling and spin/orbital polarization were allowed for, in the same way as has been described earlier.[4]

The use of full nonsphericity of the charge-density and one-electron potential is essential for accurate total energies. This is accomplished in our method by expanding charge density and potential in cubic harmonics inside nonoverlapping muffin-tin spheres and in a Fourier series in the interstitial region. In all calculations we used two energy tails associated with each basis orbital and for $6s$, $6p$, and the valence states ($7s$, $7p$, $6d$, and $5f$) these pairs were different. With this ''double basis'' approach we used a total of six energy tail parameters and a total of 12 basis functions per atom. Spherical harmonic expansions were carried out through $l_{max}=6$ for the bases, potential, and charge density. Two types of crystal structures were considered here. First, the antiferromagnetic, ferromagnetic, and nonmagnetic structures were accounted for in a two atom/cell simple tetragonal structure. Within this structure the axial c/a ratio distinguishes between fcc ($c/a=\sqrt{2}$) and body-centered cubic (bcc) ($c/a=1$). Other c/a values were also considered when studying mechanical instabilities. A special quasirandom structure model with an eight atom super cell was used to approximate a disordered magnetic structure with zero total spin moment described below (Sec. III). The sampling of the irreducible BZ was done using the special *k*-point method[12] and the number of *k* points used were up to 800 in the two atom/cell calculation and about 10 for the eight atom/cell calculation. To each energy eigenvalue a Gaussian was associated with 20-mRy width to speed up convergency.

B. KKR

The calculations we have referred to as KKR are performed using the scalar relativistic (no spin-orbit coupling) Green's-function technique based on the KKR method within the atomic sphere approximation.[13,14] Here the ASA is improved by addition of higher multipoles[14] of the charge density, and the so-called muffin-tin correction[15] to the electrostatic energy is also included. The calculations were performed for a basis set including valence $spdf$ orbitals and the semicore $6p$ state whereas the core states were recalculated at each iteration (soft-core approximation). For the electron exchange/correlation energy functional the most recent[16] local Airy gas approximation has been used. Integration over the irreducible wedge of the BZ was performed using the special *k*-point method[12] with 916 *k* points. The moments of the density of states needed for the kinetic energy and the valence charge density were calculated by integrating the Green's function on a complex energy contour (with a 2.5-Ry diameter) using a Gaussian integration technique with 30 points on a semicircle enclosing the occupied states. The equilibrium density of Pu was obtained from a Murnaghan[17] fit to about ten total energies calculated as a function of lattice constant.

The calculations were performed for nonmagnetic (NM) (spin degeneracy), ferromagnetic (FM), and antiferromagnetic (AF) magnetic configurations. Also, magnetic disorder was modeled within the CPA.[18] This was accomplished by using the so-called disordered local-moment model. In order to calculate the DLM state, one uses a random mixture of two distinct magnetic states, namely, the spin-up and spin-down configurations of the same magnetic species in the system.[19] Thus, the total energy for a system with completely randomly oriented local moments can be calculated. Here we represent a paramagnetic state of δ-Pu as a $Pu^{u}_{50}Pu^{d}_{50}$ alloy.

C. PAW

The norm-conserving pseudopotential scheme[20] has shown to be a powerful technique for performing large-scale static as well as dynamic DFT calculations using a plane-

wave basis set. Transferable pseudopotentials of this kind, however, can become computationally very expensive when applied to transition or *f*-electron systems, because of the required small core radius. A remedy to this problem was proposed by Vanderbilt in the ultrasoft pseudopotential scheme,[21] where the norm-conserving condition is relaxed and the core radius can be moved out to approximately half of the nearest-neighbor distance. In this approach, localized atom-centered augmentation charges need to be introduced. Blöchl[22] developed a generalization of the Vanderbilt ultrasoft pseudopotential and the linear augmented plane-wave[23] methods, i.e., the projector augmented wave technique. Within the PAW method, the all-electron wave functions are related to the pseudowave functions via a linear transformation.

We have performed scalar relativistic spin-polarized PAW calculations for Pu using the VASP code.[24] The electronic exchange/correlation energy functional was represented using the GGA approximation.[11] The calculations include 16 valence electrons, including the semicore $6s$ and $6p$ states with a plane-wave cutoff of 23.4 Ry. The Brillouin zone was sampled with the same grid of k points for all the spin configurations, equivalent to an $8\times8\times8$ fcc Monkhorst-Pack grid.[25]

The PAW method was checked and compared to the FPLMTO method with the same exchange/correlation functional and no spin-orbit coupling. The two methods gave nearly the same equilibrium lattice constants (within about 1%) for both the spin-polarized and spin-degenerate treatments of fcc Pu, suggesting that the PAW method is performing as well as FPLMTO for this property of Pu.

III. MAGNETIC STRUCTURE

As has been mentioned earlier,[4] DFT predicts a spontaneous formation of an ordered spin moment in δ-Pu, whereas in the ground-state α-Pu a nonmagnetic state is favored. The question of magnetism in Pu is somewhat controversial, but the most recent experiments known to these authors, addressing magnetism in Pu, are magnetic-susceptibility measurements which show a Curie-Weiss-like behavior[26,27] for δ-Pu. The susceptibility of α-Pu, however, is significantly different and essentially temperature independent.[26,27] In the latter work[27] attempts were made to fit the susceptibility of alloy-stabilized δ-Pu to a modified Curie-Weiss law. For Pu 6-at.% Ga the best fit gave an effective moment of 1.2 μ_B, whereas the renormalized value for Pu 6-at.% Ce was 1.7 μ_B.

From a DFT standpoint, the exchange splitting that gives rise to the formation of a large spin moment is very fundamental and cannot be ignored because if the theory is constrained to be spin degenerate (nonmagnetic), it fails to reproduce any known properties of δ-Pu. In the following we address the question of magnetism in δ-Pu and study several magnetic configurations and also try to represent the paramagnetic state via disordered local moments. This latter magnetic state, if stabilized, would fulfill the requirement of large exchange splitting produced by the DFT and also be consistent with the experimentally suggested Curie-Weiss magnetic susceptibility of δ-Pu.

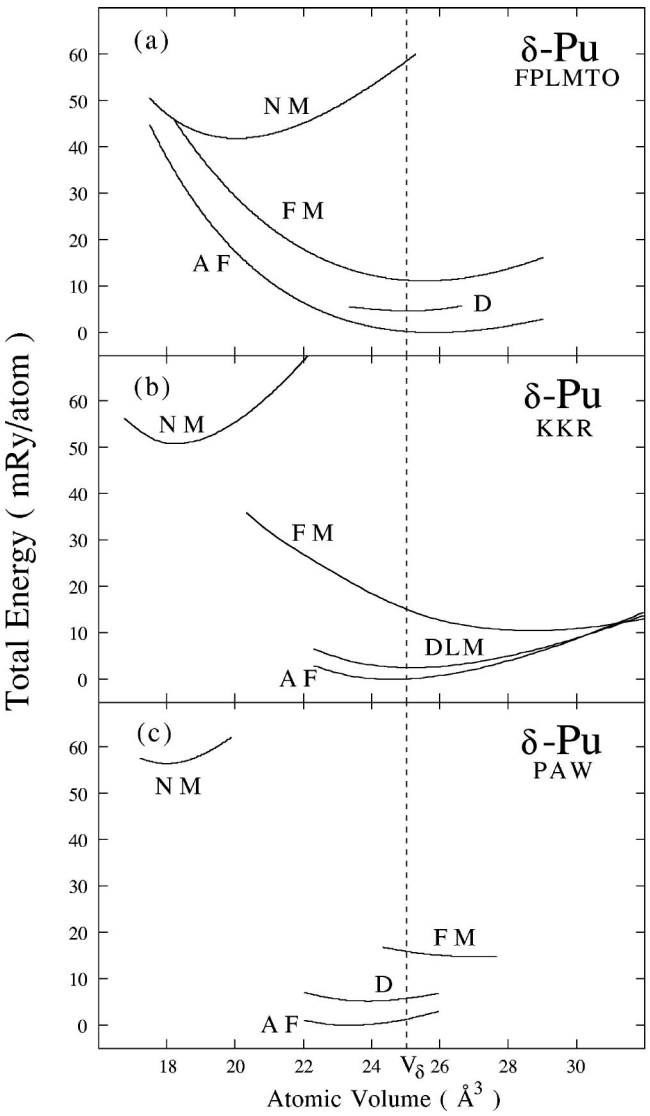

FIG. 2. FPLMTO (a), KKR (b), and PAW (c) total energies (mRy/atom) for fcc Pu in nonmagnetic (NM), ferromagnetic (FM), antiferromagnetic (AF) type-I, and disordered (D) configurations as a function of atomic volume. Dashed vertical line represents experimental equilibrium volume for δ-Pu. (Ref. 33)

In Fig. 2 we show FPLMTO [Fig. 2(a)], KKR [Fig. 2(b)], and PAW [Fig. 2(c)] total energies as a function of volume for four magnetic configurations, namely, NM, FM, AF, and disordered (D). the AF configuration is type I here, i.e., spin moments are aligned in $\langle 100\rangle$ ferromagnetic sheets with adjacent sheets having antiparallel spins and the spin quantization along the [001] direction. This type of AF ordering was predicted to be the most favorable in a previous study[4] and this fact is also confirmed here. For the FPLMTO and PAW calculations the disordered moment model consists of a special quasirandom structure with eight atoms/cell. This structure is designed[28] to mimic a perfectly random structure by reproducing its behavior for the closest neighbors around each site, deferring periodicity errors to more distant neigh-

TABLE I. Theoretical equilibrium volume (V, in Å^3), bulk modulus (B, in GPa), and site-projected spin moment (μ_s, in μ_B). For the FPLMTO calculations the orbital moment is given in parentheses. Experimental (Ref. 33) atomic volume and bulk modulus are 25.0 Å^3 and 30–35 GPa, respectively.

	FPLMTO			KKR			PAW		
Magnetic order	V	B	μ_s	V	B	μ_s	V	B	μ_s
FM	25.6	26	4.4 (−3.0)	29.0	30	5.7	27.1	24	5.2
D	25.0	42	4.3 (−3.0)	25.0	42	5.0	23.9	34	4.7
AF	25.6	35	4.5 (−3.0)	24.6	51	4.8	23.3	41	4.8

bors. For the KKR method the disorder is accomplished by the DLM approach described above.

Reviewing Fig. 2, we realize that despite the great differences in numerical implementations, our three DFT methods are in good quantitative agreement and that AF is the energetically most stable configuration closely followed by a disordered state about 2–5-mRy (~320–800 K) higher in energy. Considering the fact that the calculations assume zero temperature and δ-Pu is stable at about 600 K, this small energy difference is not sufficient to rule out any magnetic configuration. In fact, spin entropy (S_{spin}) strongly favors the disordered moment state at higher temperatures because of the large spin moment, μ_s, involved ($\mu_s \sim 5\mu_B$). As a rough estimate of this contribution we could use $S_{spin} = k_B \ln(\mu_s+1)$ for a complete disorder of spins, and this amounts to about 7 mRy at $T=600$ K.

The effect of spin-orbit coupling in fcc Pu can be appreciated by comparing the FPLMTO results with that of KKR and PAW. The NM equilibrium volumes, shown in Fig. 2, obtained from KKR and PAW calculations are significantly smaller than that of the FPLMTO calculation, i.e., the spin-orbit interaction expands that lattice in the NM treatment. This effect was first discovered and explained by Brooks[29] and was later confirmed by Söderlind *et al.*[30] Some more recent studies have come to the same conclusion.[31,32] The effect of spin-orbit coupling in the FM case is the opposite; here it leads to a smaller lattice constant as is also clear from Fig. 2. Although important for the finer details of the results, spin-orbit coupling is not essential for the quantitative behavior of δ-Pu.

In Table I we summarize the equilibrium volumes, bulk moduli, and magnetic moments obtained from our calculations. For the FPLMTO treatment the equilibrium volume, bulk modulus, and site-projected magnetic moments are about the same for the FM, AF, and D configurations and in good agreement with experiment[33] for the atomic volume and the bulk modulus. The total magnetic moment is zero for AF and D, but also the site-projected moment is rather small due to cancellation of spin and orbital contributions. The KKR calculations are more sensitive to the actual spin configuration, but for the two lowest-energy states, AF and D, the results are very similar. FPLMTO and KKR agree well with each other for the AF and D configurations although the spin moment is about 10% larger for the KKR treatment. Also the PAW equilibrium volumes, bulk moduli, and spin moments are close to both the FPLMTO and the KKR results. It is important to note that although the numerical techniques are quite different, all three methods are able to relatively accurately reproduce the anomalous δ-Pu volume and bulk modulus, especially for the AF and D configurations.

Supercell PAW calculations for several other spin configurations were performed in addition to the above investigations. Some of these included spin-restricted (nonmagnetic) sites and others a mixture of local ferromagnetic and antiferromagnetic order. These studies can be summarized as follows. (i) Configurations containing nonmagnetic sites always increase the DFT total energies significantly and predict too small volumes for δ-Pu. (ii) Local ferromagnetic alignment is always less favorable than an antiferromagnetic alignment. (iii) The AF type-I configuration, described above, is predicted to be the lowest-energy configuration.

IV. CRYSTAL STRUCTURE

In this section we study the structural stability of the two lowest-energy configurations, AF and D. Experimentally,[34] δ-Pu is known to have a very small elastic constant C' which could be interpreted as a tendency towards a tetragonal distortion of the fcc structure. Also, some fcc actinide compounds are known to show tetragonal lattice distortion induced by antiferromagnetism.[35] To investigate this for δ-Pu we display FPLMTO total energies, in Fig. 3, as a function of the c/a axial ratio at the theoretical equilibrium volume (25.6 Å^3) for AF Pu. Note that AF Pu is unstable with respect to a tetragonal distortion and that it is predicted to be body-centered tetragonal (bct) with a c/a axial ratio of about 1.5. Similar FPLMTO calculations were done (not shown) at other volumes with essentially the same result, i.e., volume relaxation effects are small and do not change the

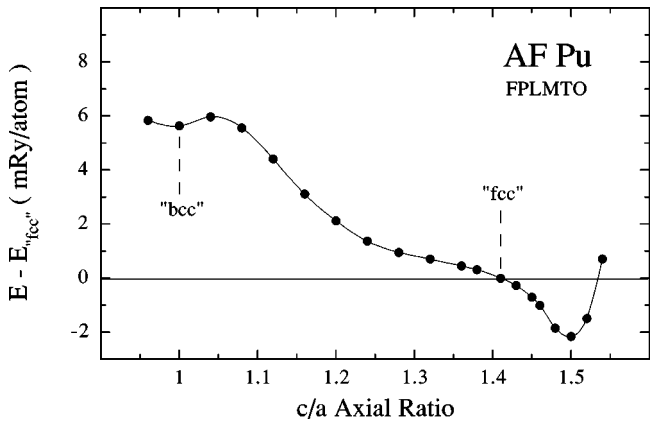

FIG. 3. FPLMTO total energy (mRy/atom) as a function of c/a axial ratio for AF δ-Pu at 25.6 Å^3.

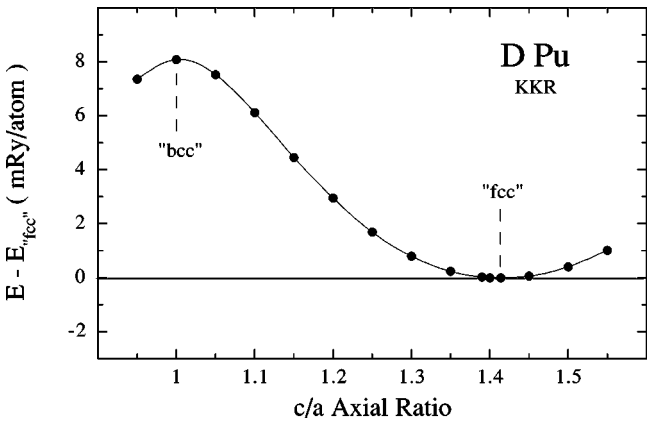

FIG. 4. KKR total energy (mRy/atom) as a function of c/a axial ratio for disordered (D) δ-Pu at 25.0 Å^3.

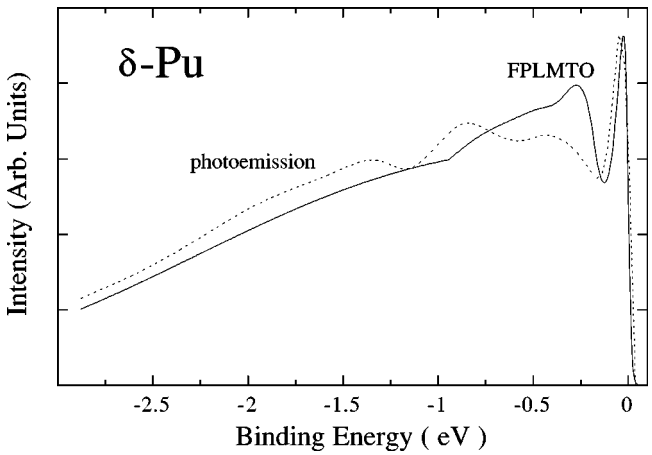

FIG. 5. Comparison of spectra (Ref. 36) (dashed line) to FPLMTO DOS (solid curve). Calculated curve is total electronic density of states that has been convoluted with lifetime broadening. (Ref. 36).

main result. This tetragonal instability of AF Pu was confirmed by both KKR and PAW calculations (not shown) performed at their respective equilibrium volumes. Next, we analyze the disordered configuration, D. Here we chose to show in Fig. 4 the results from the KKR calculations within the DLM model, of total energy as a function of the c/a axial ratio. In this figure, the volume is kept fixed to its fcc equilibrium value (25.0 Å^3), but KKR calculations at other volumes display a similar behavior. In contrast to AF Pu, δ-Pu is mechanically stable assuming disordered magnetism. This result was also confirmed by FPLMTO and PAW calculations, where the disorder was modeled by the special quasirandom structure described above.

In Fig. 4 an approximate tetragonal shear constant (C') can be calculated from the curvature of the energies close to $c/a=\sqrt{2}$. By extracting the coefficient to the harmonic term of a least-squares fit to these energies, an approximate $C'=5.0$ GPa is obtained. Although this C' only serves as an estimate, it is in good agreement with the measured[34] and very small C' (4.78 GPa). Another interesting insight from Figs. 3 and 4 is that the δ' phase (see Fig. 1), which is a bct structure with $c/a=1.33$, has a total energy less than 1-mRy (160 K) greater than the δ energy. This is consistent with the experimental phase diagram which separates these phases an amount less than 200 K. Figure 3 suggests, however, that the δ' phase is unstable with respect to a tetragonal distortion, because there is no local minimum in the energy at $c/a=1.33$.

At even higher temperature, Pu melts from the bcc (ϵ phase). Our calculations suggest the energy difference between δ-Pu and ϵ-Pu to be about 6–8 mRy which is in disagreement with estimates based on the experimental phase diagram. Clearly entropy or other effects, not accounted for in the present theory, are important in stabilizing the ϵ phase in Pu.

V. ELECTRONIC STRUCTURE

There are ongoing efforts to study the electronic structure of Pu experimentally by means of photoelectron spectroscopy.[36,37] Although not straightforward, these can be compared to calculated electronic density of states (DOS) close to and below the Fermi level (E_F). If the DOS and photoemission (PE) are incompatible, one could question the accuracy and validity of the theory. This is the case for the LDA+U method, in which there is a pseudogap[7] close to and below the E_F, where in fact the PE shows a peak in the intensity. Also a nonmagnetic LDA calculation produces a DOS in poor agreement with PE.[36] The ''constrained LDA'' technique,[6,36] as well as the DMFT,[9] however, are more consistent with PE, although neither compares perfectly with experiment.

For comparison, we show in Fig. 5 our calculated DOS obtained from FPLMTO for AF Pu at 25.0 Å^3. Here we used lifetime broadening parameters identical to those chosen by Arko *et al.*[36] who also measured the PE shown. Notice that the broadened FPLMTO DOS compares quantitatively well with photoemisson with a peak just below the E_F and a minimum at -0.2 eV (E_F is at zero). In the PE,[36] this minima is located at about -0.25 eV whereas in the PE by Havela *et al.*[37] it is located at about -0.3 eV. This feature is important because Havela *et al.* have shown that the weak satellite centered at about -0.8 eV is absent in the spectra for α-Pu and therefore indicative of the δ phase. At lower energies, below -1 eV, the convoluted FPLMTO DOS compares rather well with PE and that of the ''constrained LDA'' model,[36] whereas here the DMFT model[9] is in severe disagreement with the measurement.

We note that the DOS for AF, D, and FM are all very similar and that the comparison with photoelectron spectroscopy is not dependent upon the actual spin configuration. It is clear, however, that neglecting magnetic interactions gives rise to a DOS that is not at all compatible with the PE, as also pointed out by Arko *et al.*

VI. CONCLUSIONS

In conclusion, DFT is able to reproduce many of the anomalous properties of δ-Pu, when magnetic exchange interaction is taken into account. This interaction is essential to the theory, and if ignored severely erroneous behavior of the

metal is predicted. The lowest zero-temperature DFT energy is obtained for antiferromagnetic type-I ordering of spin moments with a magnitude close to $5\mu_B$. Energetically very competitive is a disordered magnetic structure with a somewhat smaller spin moment. FPLMTO also predicts a large antiparallel orbital moment that nearly cancels the spin moment. The resulting total moment is about $1.3\ \mu_B$–$1.5\ \mu_B$, which is close to an experimentally estimated effective moment,[27] but it is unclear if these can be directly compared.

We suggest that the AF ordering does not occur at temperatures where δ-Pu is stable because we have shown that this ordering destabilizes δ-Pu with respect to a tetragonal distortion. Instead, we propose that δ-Pu is a *disordered magnet*. At zero temperature the DFT energies for AF and random ordering are close but at higher temperatures the great magnitude of the spin moments implies that spin entropy would strongly disfavor ordering of the spins. In addition, and in contrast to the AF ordering, random ordering of the spins supports mechanical stability of δ-Pu.

Experimentally, δ-Pu is unstable below about 600 K, where fcc transforms to a lower-symmetry structure (α-Pu). This behavior is here explained by the inherent tendency toward magnetic ordering in δ-Pu at lower temperatures followed by a mechanical instability of the fcc phase. It is well known, however, that a small amount of Al or Ga (for example) can stabilize δ-Pu to lower temperatures. In the near future, we plan to study the effects of alloying on the magnetic properties of δ-Pu and the stability of the fcc phase.

ACKNOWLEDGMENTS

We would like to thank A.V. Ruban, P.A. Korzhavyi, and O. Eriksson for helpful discussions. This work was performed under the auspices of the U.S. Department of Energy by the University of California Lawrence Livermore National Laboratory under Contract No. W-7405-Eng-48.

[1] D. A. Young, *Phase Diagrams of the Elements* (University of California, Berkeley, 1991).
[2] P. Söderlind and C. S. Nash, in *Advances in Plutonium Chemistry 1967–2000*, edited by D. C. Hoffman (American Nuclear Society, LaGrange Park, IL, 2002), p. 6.
[3] P. Söderlind, Phys. Rev. B **66**, 085113 (2002).
[4] P. Söderlind, Europhys. Lett. **55**, 525 (2001).
[5] M. Penicaud, J. Phys.: Condens. Matter **9**, 6341 (1997).
[6] O. Eriksson, J.M. Wills, D. Becker, and A.V. Balatsky, J. Alloys Compd. **287**, 1 (1999).
[7] J. Bouchet, B. Siberchicot, F. Jollet, and A. Pasturel, J. Phys.: Condens. Matter **12**, 1723 (2000).
[8] S.Y. Savrasov and G. Kotliar, Phys. Rev. Lett. **84**, 3670 (2000).
[9] S.Y. Savrasov, G. Kotliar, and E. Abrahams, Nature (London) **410**, 793 (2001).
[10] J.M. Wills and B.R. Cooper, Phys. Rev. B **36**, 3809 (1987); D.L. Price and B.R. Cooper, *ibid.* **39**, 4945 (1989).
[11] J.P. Perdew, J.A. Chevary, S.H. Vosko, K.A. Jackson, M.R. Pederson, and D.J. Singh, Phys. Rev. B **46**, 6671 (1992).
[12] D.J. Chadi and M.L. Cohen, Phys. Rev. B **8**, 5747 (1973); S. Froyen, *ibid.* **39**, 3168 (1989).
[13] O. Gunnarsson, O. Jepsen, and O.K. Andersen, Phys. Rev. B **27**, 7144 (1983).
[14] A.V. Ruban and H.L. Skriver, Comput. Mater. Sci. **15**, 119 (1999).
[15] N.E. Christensen and S. Satpathy, Phys. Rev. Lett. **55**, 600 (1985).
[16] L. Vitos, B. Johansson, J. Kollar, and H.L. Skriver, Phys. Rev. A **61**, 052511 (2000); Phys. Rev. B **62**, 10 046 (2000).
[17] F.D. Murnaghan, Proc. Natl. Acad. Sci. U.S.A. **30**, 244 (1944).
[18] J.S. Faulkner, Prog. Mater. Sci. **27**, 1 (1992).
[19] B.L. Györffy, A.J. Pindor, G.M. Stocks, J. Stauntin, and H. Winter, J. Phys. F: Met. Phys. **15**, 1337 (1985).
[20] D.R. Hamann, M. Schlüter, and C. Chiang, Phys. Rev. Lett. **43**, 1494 (1979).
[21] D. Vanderbilt, Phys. Rev. B **41**, 7892 (1990).
[22] P.E. Blöchl, Phys. Rev. B **50**, 17 953 (1994).
[23] D. J. Singh, *Planewaves, Pseudopotentials, and the LAPW Method* (Kluwer, Boston, 1994).
[24] G. Kresse and J. Hafner, Phys. Rev. B **47**, 558 (1993); G. Kresse and J. Furthmüller, *ibid.* **54**, 11 169 (1996); G. Kresse and D. Joubert, *ibid.* **59**, 1758 (1999).
[25] H.J. Monkhorst and J.D. Pack, Phys. Rev. B **13**, 5188 (1976).
[26] C.E. Olsen, A.L. Comstock, and T.A. Sandenaw, J. Nucl. Mater. **195**, 312 (1992).
[27] S. Meot-Reymond and J.M. Fournier, J. Alloys Compd. **232**, 119 (1996).
[28] A. Zunger, S.-H. Wei, L.G. Ferreira, and J.E. Bernard, Phys. Rev. Lett. **65**, 353 (1990).
[29] M.S.S. Brooks, J. Phys. F: Met. Phys. **13**, 103 (1983).
[30] P. Söderlind, L. Nordström, L. Yongming, and B. Johansson, Phys. Rev. B **42**, 4544 (1990).
[31] P.M. Oppeneer, T. Kraft, and M.S.S. Brooks, Phys. Rev. B **61**, 12 825 (2000).
[32] L. Nordström, J.M. Wills, P.H. Andersson, P. Söderlind, and O. Eriksson, Phys. Rev. B **63**, 035103 (2001).
[33] R. L. Moment, in *Plutonium and Other Actinides*, edited by H. Blank and R. Lindner (North-Holland, Amsterdam, 1976), p. 687.
[34] H.M. Ledbetter and R.L. Moment, Acta Metall. **24**, 891 (1976).
[35] G.H. Lander and M.H. Mueller, Phys. Rev. B **10**, 1994 (1974).
[36] A.J. Arko, J.J. Joyce, L. Morales, J. Wills, J. Lashley, F. Wastin, and J. Rebizant, Phys. Rev. B **62**, 1773 (2000).
[37] L. Havela, T. Gouder, F. Wastin, and J. Rebizant, Phys. Rev. B **65**, 235118 (2002).